International Journal of Computer Science and Software Engineering (IJCSSE), Volume 5, Issue 5, May 2016
ISSN (Online): 2409-4285 www.IJCSSE.org Page: 89-96

PSO Based Diagnosis Approach for Surface and Components Faults in Railways

Orhan Yaman[1], Mehmet Karakose[2], Erhan Akin[3]

[1, 2, 3] Computer Engineering Department, Firat University, Elazig, Turkey

[1]*orhanyaman@firat.edu.tr*, [2]*mkarakose@firat.edu.tr*, [3]*eakin@firat.edu.tr*

ABSTRACT

Railway transport is a type of transport which is commonly used today. Rail line must be robust due to the heavy structure of the railway vehicles. Components constituting the rail line are very important to prevent the disruption of transportation. In this study, faults are determined by monitoring the rail and fastening components constituting the railway. Test vehicle was used to get experimental data. The left and right rails were viewed from different angles by four cameras placed on the test vehicle. Status monitoring and fault detection were performed by applying image processing and particle swarm optimization methods to the images taken. Rail surface was determined by taking the right and left images of rail line from the right and left cameras from different angles. Images taken from the right and left cameras were assembled for the detection of faults in the rail surface. Image matching was performed during the detection of fastening components and the rail surface. Matching was performed for each image taken from the camera by taking into account the correlation coefficient. In the determination of rail surface, template image and similarity were measured by taking specific sections on the image respectively. After template image and similarity ratios of all sections taken from the image were calculated, the sectional image with the highest correlation coefficient was determined as the rail surface. Sections were taken randomly from the image during the detection rail component. The correlation coefficient of the template image was calculated with the sections taken. Correlation coefficient was used as the coherence function in the particle swarm optimization, and fastening components were determined. Condition monitoring was performed by combining the detection results obtained.

Keywords: *Condition Monitoring, Railway, Image Processing, Rail Component Detection*.

1. INTRODUCTION

Railway transport is an important type of transport used for many years. It has become a popular type of transport with the increase of transport quality and safety and the acceleration of the railway vehicles in recent years. Components on the railway line should be monitored at regular intervals to ensure continuous transport security [1]. Railway components are generally monitored in two different ways. Structures developed for contact monitoring method are generally slow and must be in contact with the railway components [2]. Such methods are not preferred today; instead of this, non-contact condition monitoring methods are preferred [3-5]. Railway line is monitored in a non-contact manner by the cameras used in these methods, and faults that occur in the railway line are determined by the developed image processing algorithms [6-10]. Such methods reduce the workload by working faster. Sun et al. [11] developed an automatic inspection tool for rail systems. They examined the pattern and shape of the rail with a laser scanner. In the method developed, faults occurring on the rail components were determined and information such as repair and replacement of rails are achieved. Contact monitoring method given in the literature is a non-preferred method due to its cost.

When the studies in the literature were analyzed, it was observed that non-contact condition monitoring methods were more preferred, and that many approaches were presented for the condition monitoring. Quingyong et al. [12] made real time detection for faults occurring on rail surface by developing an image processing based non-contact method. Part extraction was made from the rail images, and rail surface was removed. Surface faults were found on the rail surfaces removed by contrast enhancing method. This method finds the surface faults only by detecting the rail surface. Limin et al. [13] proposed a method for the detection of faults that occur in the rail surface using machine vision techniques. They determined the roughnesses and cracks formed on the rail surface by image processing. Edge extraction methods were used for feature extraction on the image.

Trinh et al. [14] proposed a method for the detection of railway components by using distance measuring equipment, GPS sensor and 4 cameras. In the method proposed, image processing based automatic control

system was developed. Hough determined the horizontal lines using the transformation for the detection of connection plates and other components. Edge extraction was made using sobel edge extraction, and also fastening components and fastening plates were determined in the method proposed and their positions were determined. The general architecture of the method developed in this study proposed is given in Figure 1.

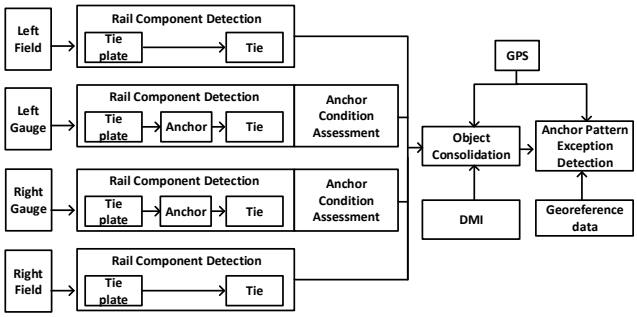

Fig. 1. General architecture of the railway control system in the literature [14].

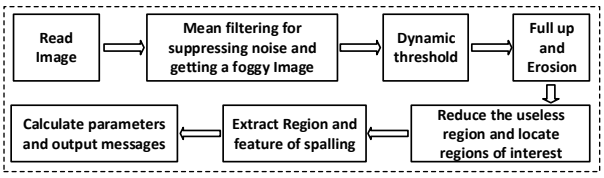

Fig. 2. Flow chart of spalling image processing [15].

In the literature given in Figure 1, images were taken from different locations on the railway using four cameras. Fastening components were determined by performing image processing on the images taken from cameras.

In their study, Liu et al [15] proposed a machine vision based method for the inspection of rail surface faults. The proposed method is seen in Figure 2. Spalling faults, cracks and many other faults formed on the rail surface were analyzed. Image segmentation and some feature extraction methods were applied to the railway image. Dynamic matching was performed by removing the faulty region from the image. The sizes of the cracks formed on the rail surface were calculated, and fault evaluation was performed.

Feng et al. [16] proposed a vision-based method for the detection of railway fasteners, sleepers and the rail. Component detection was performed applying image processing method on images taken from the railway. The proposed method for three different fastening components was tested.

In the proposed method, images 560 x 900 pixels in size were taken using experimental setup. The position detection, classification and points rating of the fastening components were performed on the images taken. Rail and sleeper detection was performed using line segment detector LSD algorithm on the images. The experimental setup used in the proposed method is given in Figure 3, and the flow chart of the data processing module is given in Figure 4.

In the proposed method, detection of the fastening components was performed by 95.2% success. 57124 images were taken using a 110 km long railway line to test the proposed method. A total of 399078 fastening components were determined on the images taken. The size of the fastening components determined on the images is 110 x 160 pixels. Results were obtained by testing in other algorithms used in the proposed method.

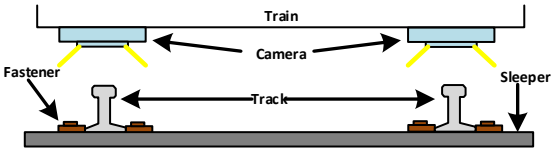

Fig. 3. Experimental setup used in the proposed method [16].

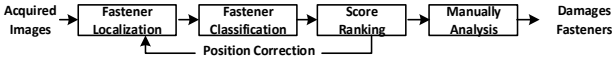

Fig. 4. Flow chart of the data processing module [16].

In their study, Wohlfeil et al. [17] railway line crossings detection was performed to prevent the collision of trains on the railway line. Image of the railway line was taken from the camera placed on the locomotive. Railway components were determined from the image taken, and line crossings were determined. The success of the proposed method was observed by being tested in different weather conditions in different regions.

In this study, the railway line was monitored with the developed algorithms. Through four cameras used, rail surface and fastening components on the railway line were determined, and the sizes of faults occurring on rail surface were calculated. By combining the results obtained, condition monitoring and inferences of the railway line were performed. Basic image processing methods, image matching and particle swarm optimization algorithms were used in the method developed. They were matched with the images taken from the camera using the template images representing the fastening component and the rail surface. While matching the rail surface, template image is scanned over the entire image and the area with high correlation coefficient is determined as the rail surface. Particle swarm optimization was used while determining the railway components. The results obtained by examining the studies in the literature were compared with the proposed method.

2. PROPOSED METHOD

In this study, railway components were determined using image processing methods. Faults occurred on the determined rail surface and fastening components were identified, and condition monitoring was conducted. Block diagram of the proposed method is given in Figure 5.

In the block diagram given in Figure 5, images were taken by four cameras from the railway line. Rail surface determination was performed for the image taken from each camera. Images were combined by considering the rail surfaces determined right and left camera of the right and left rails, and rail surface fault determination was performed on the imaged combined. Also, fastening component determination was performed using particle swarm optimization. Condition monitoring was performed on the railway line combining the results obtained. Flow chart of proposed method for the determination of rail surface faults and railway component is given in Figure 6.

Rail surface template image which is in 30x320 size used in the proposed method is given in Figure 7.a. Template image was matched with the sections in 30x320 size taken from the railway image in 240x320 size in Figure 7.b. This process is repeated until the last pixel on the image. The graph indicating the correlation values of the sections on the entire image is seen in Figure 7.c. After the matching process, section with the highest correlation value is determined as the rail surface [18-22]. The rail image surface determined is given in Figure 7.d.

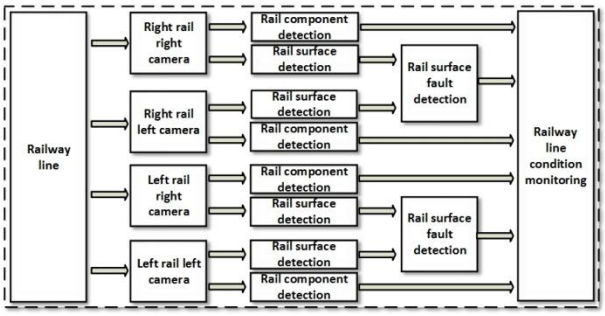

Fig. 5. Block structure of the proposed method.

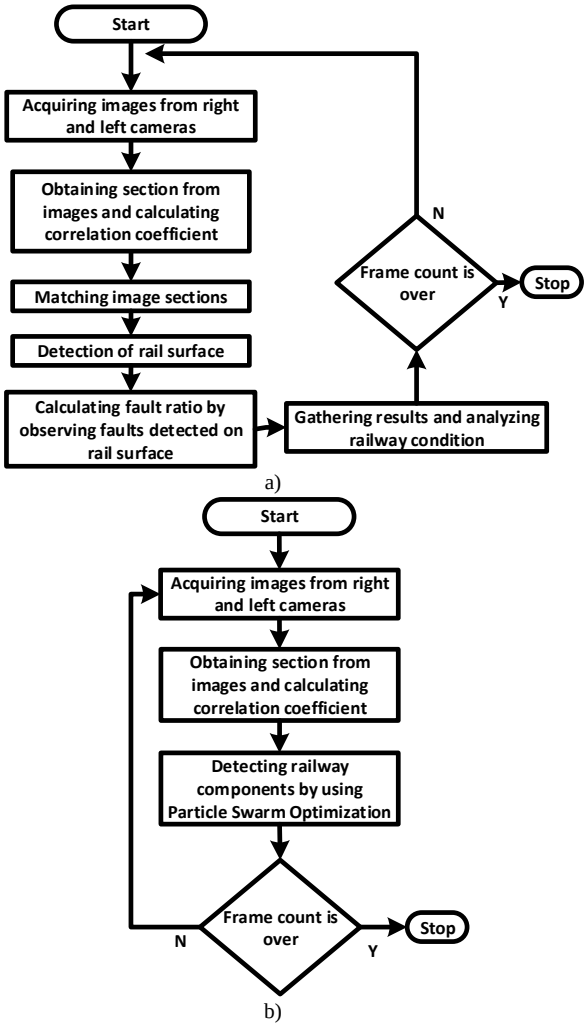

Fig. 6. Flow charts of the proposed method a) Rail surface determination method b) Rail component determination method.

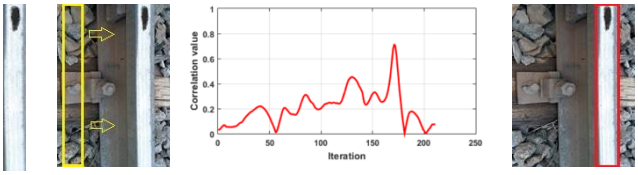

Fig. 7. Determination of the rail surface by using correlation coefficient to the railway image a) Template image b) Railway image c) Graph showing the correlation value calculated for each section taken d) Determination of the rail surface on the image.

The operation for finding the similarity of each other by examining "M, N" image matrices is given in equation 1.

$$r = \frac{\sigma_{TS}}{\sigma_{TS}} = \frac{\sum_{i=1}^{R}\sum_{j=1}^{C}(g_T(i,j)-\bar{g}_T)(g_S(i,j)-\bar{g}_S)}{\left(\sum_{i=1}^{R}\sum_{j=1}^{C}\left(g_T(i,j)-\bar{g}_T\right)\right)^2 \sum_{i=1}^{R}\sum_{j=1}^{C}\left(g_S(i,j)-\bar{g}_S\right)\Big)^2\Big\}^{1/2}} \quad (1)$$

In equation 1, "r" represents the correlation coefficient, "σ_I" and "σs" represent the standard deviation of gray values in template and search window, "σ_{IS}" represents the covariance of gray values in search windows, "g_I" and "gs" represent the gray values in template and search window, "$\check{g}_I$" and "$\check{g}s$" represent the average gray values, "R" and "C" represent the number of rows and columns in the search window. Similarity between two images will be more to extent how much nearer is the correlation coefficient between the two images to 1 [23]. It is compared with the sections on the image taken from camera by using a template image in the determination of railway component. In the determination of railway component, particle swarm optimization was preferred instead of scanning the template image on the entire image. Faster results are obtained using particle swarm optimization. This algorithm is a population-based optimization method to find the optimal results to nonlinear problems by being inspired by the movements of birds, fish and other flocks [24]. Particle swarm optimization firstly generates individuals, each of whom offers candidate solution, to find the optimal or near optimal solution. A flock is composed of "N" pieces of particle moving in "D" dimensional search space. The position of "i." at the "t" moment is used in assessing the quality of the particle for any search or optimization problem and represent the candidate solution or solutions. It is represented by "$x_i(t)= (x_{i1}, x_{i2}, \ldots, x_{iD})$". Here, "$x_{i,n}(t) \in [l_n, u_n]$, $1 \leq n \leq N$ l_n" and "u_n" indicate the upper and lower limits of "n." dimension, respectively. Each particle adjusts its position to the best position in the flock during searching and also benefits from previous experience. Namely, it adjusts its position according to two factors: personal best position indicated as "$p_{i,j} = (p_{i1}, p_{i2}, \ldots, p_{iD})$" (pbest) and the best position in the entire flock indicated as "$p_g = (p_{g1}, p_{g2}, \ldots, p_{gD})$" (gbest). The speed in "t." iteration is indicated with "$v_i(t) = (v_{i1}, v_{i2}, \ldots, v_{iD})$" and limited with "$v_{imax} = (v_{imax1}, v_{imax2}, \ldots, v_{imaxD})$". The next speed and position of the particle is calculated according to equation 2 and equation 3.

$$v_{i,j}(t+1) = wv_{i,j}(t) + c_1 r_{1,j}(t)\left(pbest_{i,j}(t) - x_{i,j}(t)\right) + c_2 r_{2,j}(t)\left(gbest_i(t) - x_{i,j}(t)\right) \quad (2)$$

$$x_i(t+1) = x_i(t) + v_i(t+1) \quad (3)$$

The algorithm uses two independent random sequences, "$r_1 \sim U(0, 1)$ ve $r_2 \sim U(0, 1)$." In addition, "c_1" and "c_2" coefficients are "$0 < c_1, c_2 \leq 2$" learning factors. Here, "$w \in [0.8, 1.2]$" is the inertia weight and original particle swarm optimization speed update equation is "$w = 1$". Fastening component determination stages on a sample image using particle swarm optimization is given in Figure 8.

In Figure 8, stages of the railway component determination with particle swarm optimization on a sample image taken from the camera are given. Template image in 90x75 size used for matching is given in Figure 8.a. Image in 240x320 size taken from the camera is given in Figure 8.b. In Figure 8.c, Figure 8.d and Figure 8.e, results obtained during the iteration in particle swarm optimization are given. Graph showing the correlation value as a result of 20 iteration is given in Figure 8.f.

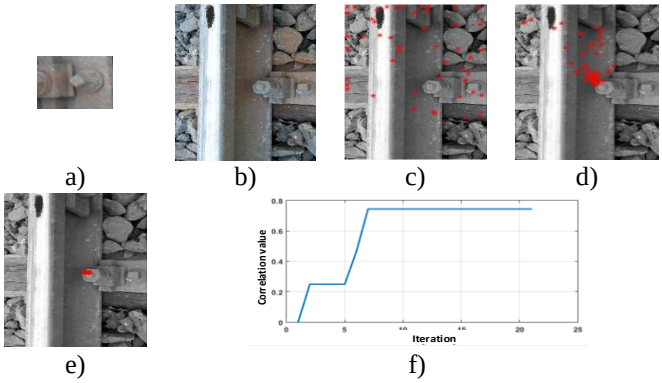

Fig. 8. Determination of railway component using the particle swarm optimization a) Template image b) Image taken from the camera c) 1. Iteration d) 6. Iteration e) 10. Iteration f) Graph showing the correlation values in 20 iterations with particle swarm optimization

3. EXPERIMENTAL RESULTS

In Figure 9.a, as it is seen in the experimental structure, four cameras were fixed on the image receiving vehicle with an angle of 45 degrees. Cameras were connected to a computer and image transfer was performed. Images taken were processed by the proposed method, and condition monitoring results were achieved for the railway line. The proposed method was tested on two different railway lines with wooden and concrete sleepers. Sample images taken from the railway line with wooden sleepers and the results obtained are given in Figure 10.

In Figure 10.a, railway images taken from four cameras are seen. Images were obtained by taking from left rail left camera, left rail right camera, right rail left camera and right rail right camera. By applying the proposed method on these images, railway components and rail surfaces were determined as in Figure 10.b. Then, images were combined considering rail surfaces. By changing binary colour from the gray image of right and left rail surfaces, faults occurring on the rail surfaces were determined. The proposed method was also tested on the railway line with a concrete sleeper. Sample images taken during the testing process are given in Figure 11.

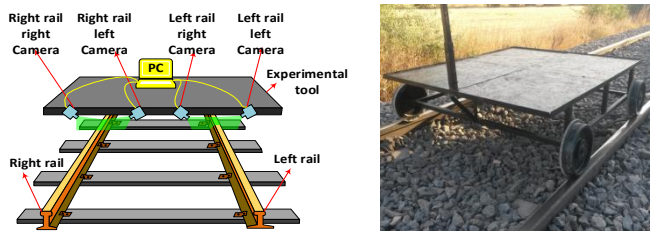

a) b)

Fig. 9. Experimental structure and image taking device used in image taking a) Experimental structure b) Image taking device.

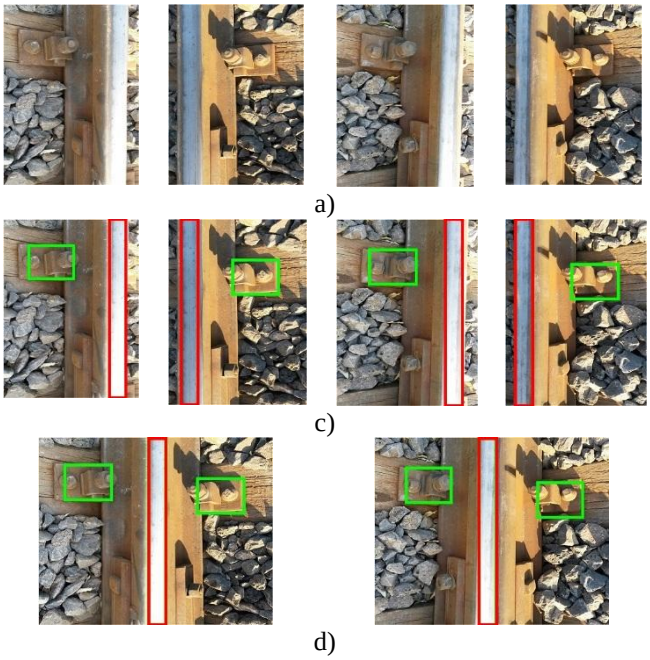

a) c) d)

Fig. 10. Images taken from the railway line with wooden sleepers and the implementation of the proposed method to these images a) Images taken from four cameras b) Determination of the rail surface and railway components on the images c) Combining images considering rail surfaces

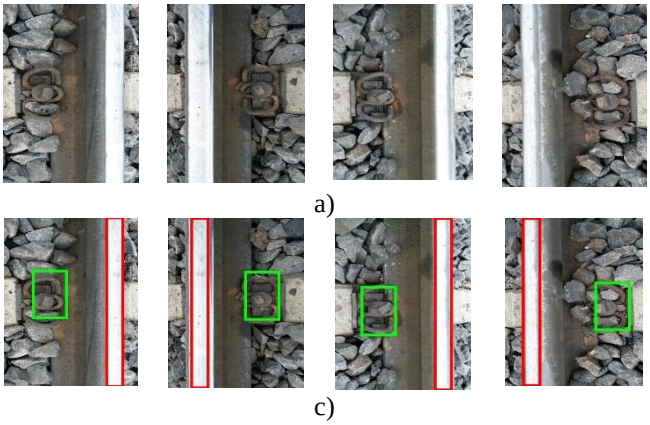

a) c)

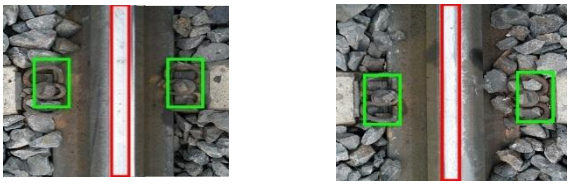

d)

Fig. 11. Images taken from the railway line with concrete sleeper and the implementation of the proposed method to these images) Images taken from four cameras b) Determination of the rail surface and railway components on the images c) Combining images considering rail surfaces.

Fastening components are different in the images given in Figure 10 and Figure 11. In Figure 10, "K" fastening type and material were used in wooden sleeper. In Figure 11, "HM" fastening type and materials were used. In Figure 12, graph indicating the correlation values for the determination of fastening component on the railway line with wooden and concrete sleeper along 100 frame, and the correlation values for the determination of rail surface are given.

Correlation values obtained in the determination of fastening component of railway with wooden sleeper are given in Figure 12.a. Correlation values were calculated for 100-frame images taken from four cameras. Similarly, results in Figure 12.b in the concrete sleeper were obtained. Additionally, correlation values obtained also in the determination of rail surface are given in Figure 12.c. When the graphs are examined in Figure 12, it is seen that correlation values vary between 0 and 0.8. In the proposed method, a threshold value was determined for the determination of fastening component and the rail surface. The high or low threshold affects the success rate of the proposed method. Threshold value table is given in Table 1 for the determination of fastening component in wooden and concrete sleepers and also the rail surface.

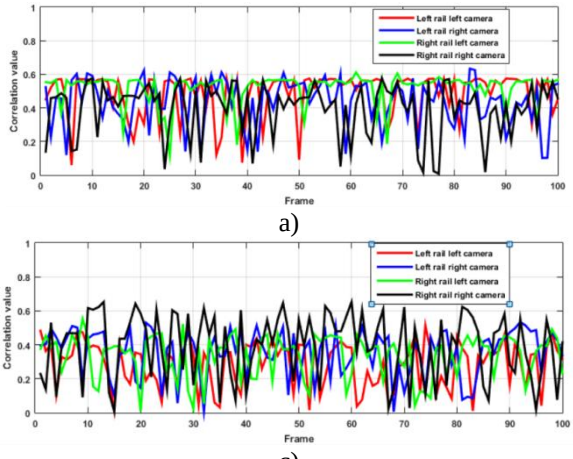

a) c)

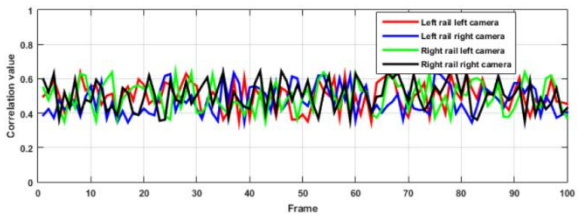

d)

Fig. 12. Determination of fastening component for the railway line with wooden and concrete sleepers, and the correlation values for the rail surface a) Wooden sleeper b) Concrete sleeper c) Rail surface

Table 1: Change of threshold value and the success rate in the proposed method

	Success Rate (%)		
	Treshold	***Average***	***Standard Deviation***
Treshold values for wooden sleeper	0,2	89,4	3,16
	0,3	79,4	3,65
	0,4	63,4	3,27
	0,5	52,8	4,36
Treshold values for concrete sleeper	0,2	80,1	3,2
	0,3	73,8	3,7
	0,4	62,2	3,7
	0,5	41,0	4,9
Treshold values for rail surface detection	0,2	98,1	1,3
	0,3	92,3	2,9
	0,4	82,5	3,5
	0,5	52,5	4,1

As it is seen in Table 1, success rate increases to the extent how small is the threshold value selected. Determining the threshold value as 0.2 means that determination has been performed. Threshold value was selected as 0.4 for the proposed method. When the threshold value was selected as 0.4, determination of fastening component was successful by 63.4% for wooden sleeper, determination of fastening component was successful by 62.2% for concrete sleeper, and determination of fastening component was successful by 82.5% for the rail surface. Due to the fact that ballasts are on sleeper during the determination of fastening component and are excessively affected by environmental conditions, success rate is lower than the determination of rail surface. When the threshold value is applied, 'Logic 1' fastening component could not be determined for fastening component determination, and 'Logic 0' means that fastening component has been determined. While condition monitoring is performed, the number of black pixels in the image is taken into account by converting rail surfaces to binary-based image. Results obtained in the proposed method for the combination of results and condition monitoring are given in Figure 13.

In Figure 13, 16 pieces of undetectable fastening components were found for 100 frame images "in the determination of left rail and left camera", and 84 pieces of determined fastening components were found. The number of undetectable fastening component for "the determination of left rail and right camera" is 12, it is 4 for "the determination of right rail left camera, and it is 22 for "the determination of right rail right camera". In addition, rail surface fault ratio in each frame of the determined rail surfaces is seen in Figure 13. Rail surface faults formed along 100 frame are within the range of 0% to 10% in the left rail surface condition and the right rail surface condition graphs. These values show that there is no excessive fault on the rail surface and that the rail surface is robust.

In this study, the proposed method was tested in a computer with intel i7 processor, 2.00 GHz speed, 8 GB of RAM and 64 operating system. Working hours of the method proposed for the determination of fastening component and the rail surface are given in Table 2.

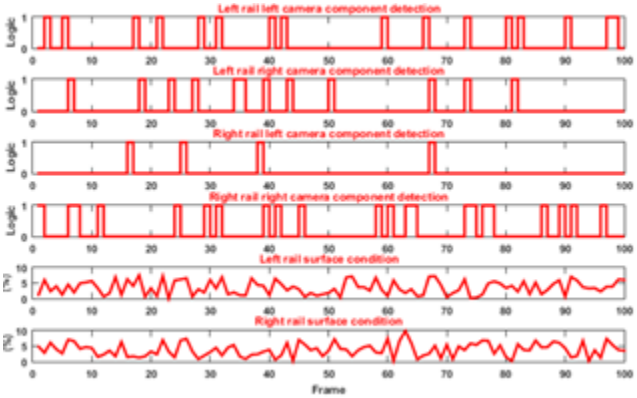

Fig. 13. Combination of results and condition monitoring.

Table 2: Working hours of the method proposed

Method	***Average time (ms)***	***Standard deviation (ms)***
Tie component detection method	313,39	2,26
Rail surface detection method	113,76	2,07
Tie component detection method and Rail surface detection method	427,15	2,16

4. CONCLUSIONS

In this study, rail surface faults which are one of the important faults that occur in the railway line and the fastening component elements were investigated. Many types of faults occur on the rail surface. When these faults are not determined earlier and repaired, bigger

faults occur and this leads to the occurrence of accidents. Also, it causes rails to be fixed to sleepers as a result of the dislodgement or loosening of fastening components. Thus, railway vehicles may be derailed many major accidents may occur. In the proposed method, rail surface and fastening components are monitored to avoid the occurrence of accidents occurring on the railway and troubles in transportation. A test vehicle was developed for this, and four cameras were placed on them. Determination of rail surface and fastening components were performed by taking images from four cameras while moving on the railway line with the test vehicle. Image matching was performed in the proposed method. Using template images representing the rail surface and the fastening component, rail surface and the fastening component were determined by image matching. Correlation values were used for image matching process. Rail surface determination was performed by comparing the sections obtained from image taken from the camera and the template image. In the fastening component determination, the process of determination was accelerated using particle swarm optimization. When the available studies in the literature were analyzed, it was seen that while rail surface determination was performed in some studies, fastening component determination was performed in some studies. In this study, railway line was monitored as a whole by using four cameras and taking images from different angles. In addition, the proposed method determines both the rail surface faults and fastening components.

Acknowledgments

This work was supported by the TUBITAK (The Scientific and Technological Research Council of Turkey) under Grant No: 114E202.

REFERENCES

[1] A. Berry, B. Nejikovsky, X. Gilbert, and A. Jajaddini, “High speed video inspection of joint bars using advanced image collection and processing techniques,” In Proc. of World Congress on Railway Research, 2008.

[2] C. González-Nicieza, M. I. Álvarez-Fernández, A. Menéndez-Díaz, A. E. Álvarez-Vigil, and F. Ariznavarreta-Fernández, “Failure analysis of concrete sleepers in heavy haul railway tracks,” Engineering Failure Analysis, 15(1), 2008, pp. 90-117.

[3] S. V. Sawadısavı, “Development of Machine-Vision Technology for Inspectıon of Railroad Track,” Graduate College of the University of Illinois at Urbana-Champaign, 2010.

[4] M. Maqsood, A. Javed, and N. Majeed, “A Novel Algorithm for Railway Tracks Detection using Satellite Imagery,” International Journal of Computer Applications, 2013, pp. 13-17.

[5] O. Yaman, M. Karakose, E. Akin, and I. Aydin, “Image processing based fault detection approach for rail surface,” In Signal Processing and Communications Applications Conference (SIU), 2015, pp. 1118-1121.

[6] E. Karakose, M. T. Gencoglu, M. Karakose, O. Yaman, I. Aydin, and E. Akin, “A new arc detection method based on fuzzy logic using S-transform for pantograph–catenary systems,” Journal of Intelligent Manufacturing, 2015, pp. 1-18.

[7] L. F. Molina, E. Resendiz, J. R. Edwards, J. M. Hart, C. P. Barkan,and N. Ahuja, “Condition Monitoring of Railway Turnouts and Other Track Components Using Machine Vision” TRB 11-1442, 2010.

[8] X. Gibert, V. M. Patel, and R. Chellappa, “Robust fastener detection for autonomous visual railway track inspection,” IEEE Winter Conference on In Applications of Computer Vision (WACV), 2015, pp. 694-701.

[9] X. Giben, V.M. Patel, and R. Chellappa, “Material classification and semantic segmentation of railway track images with deep convolutional neural networks,” Intern. Conf. on In Image Processing, 2015, pp. 621-625.

[10] Q. Li, Z. Zhong, Z. Liang, and Y. Liang, “Rail Inspection Meets Big Data: Methods and Trends,” Intern. Conf. on In Network-Based Inf. Sys., 2015, pp. 302-308.

[11] B. Sun, J. Zhuang, J. Lin, Q. Zhang, and S. Chen, “Research on the new rail auto-inspection system,” IET International Conference on Smart and Sustainable City (ICSSC), 2011, pp. 1-4.

[12] L. Qingyong, and R. Shengwei, “A Real-Time Visual Inspection System for Discrete Surface Defects of Rail Heads,” IEEE Transactions on Instrumentation and Measurement, vol. 61, 2012, pp. 2189-2199.

[13] C. Limin, L. Yin, and W. Kaimin, “Inspection of rail surface defect based on machine vision system,” 2nd International Conference on Information Science and Engineering (ICISE), 2010, pp. 3793 – 3796.

[14] H. Trinh, N. Haas, L. Ying, C. Otto, and S. Pankanti, “Enhanced rail component detection and consolidation for rail track inspection,” IEEE Workshop on Applications of Computer Vision (WACV), 2012, pp. 289–295.

[15] Z. Liu, W. Wang, X. Zhang, and W. Jia, “Inspection of rail surface defects based on image processing,” International Asia Conference on In Informatics in Control, Automation and Robotics, vol. 1, 2010, pp. 472-475.

[16] H. Feng, Z. Jiang, F. Xie, P. Yang, J. Shi, and L. Chen, “Automatic fastener classification and defect detection in vision-based railway inspection systems,” Trans. on Instr. and Measurement, 2014.

[17] J. Wohlfeil, “Vision based rail track and switch recognition for self-localization of trains in a rail

network," IEEE In Intelligent Vehicles Symposium, 2011, pp. 1025-1030.
[18] S. Zheng, X. Chai, X. An, and L. Li, "Railway Track Gauge Inspection Method Based on Computer Vision," International Conference on Mechatronics and Automation (ICMA), 2012, pp. 1292-1296.
[19] A. Mazzù, L. Solazzi, M. Lancini, C. Petrogalli, A. Ghidini, and M. Faccoli, "An experimental procedure for surface damage assessment in railway wheel and rail steels," Wear, vol. 342, 2015, pp. 22-32.
[20] H. Trinh, N. Haas, and S. Pankanti, "Multisensor evidence integration and optimization in rail inspection," 21st International Conference on Pattern Recognition (ICPR), 2012, pp. 886–889.
[21] L. Ying, T. Trinh, N. Haas, C. Otto, and S. Pankanti, "Rail Component Detection, Optimization and Assessment for Automatic Rail Track Inspection," Trans. on Intelligent Transportation Sys., 2014, pp. 760–770.
[22] R. A. Khan, S. Islam, and R. Biswas, "Automatic Detection of Defective Rail Anchors," IEEE 17th International Conference on Intelligent Trasportation Systems (ITSC), 2014, pp. 1583–1588.
[23] B. Zitova, and J. Flusser, "Image registration methods: a survey. Image and vision computing," 21(11), pp. 977-1000, 2003.
[24] B. Alatas, and E. Akin, "Multi-objective rule mining using a chaotic particle swarm optimization algorithm," Knowledge-Based Systems, 22(6), 2009, pp. 455-460.

AUTHOR PROFILES:

Orhan Yaman born in Elazig, Turkey, in 1990. He received B. S. degree in computer engineering from Firat University, Elazig, Turkey, in 2012, the M. S. degree in computer engineering from Firat University, Elazig, Turkey, in 2014, respectively and he started the Ph. D. program in computer engineering from Firat University, Elazig, Turkey, in 2014. He works as expert in the Computer Center, Firat University, Elazig, Turkey. His research interests are image processing, fault diagnosis, computer vision, railway inspection systems and fuzzy systems.

Mehmet Karakose received the B. S. degree in electrical engineering from Firat University, Elazig, Turkey, in 1998, the M. S. degree in computer engineering from Firat University, Elazig, Turkey, in 2001, respectively, and the Ph. D. degree in electrical engineering (computer engineering) from Firat University, Elazig, Turkey, in 2005. He is currently an associate professor doctor in the Department of Computer Engineering, Firat University, Turkey. He was a research assistant at Computer Engineering Department, Firat University from 1999 to 2005. His research interests include fuzzy systems, intelligent systems, simulation and modeling, fault diagnosis, computer vision, railway inspection systems, and photovoltaic systems. Assoc. Prof. Karakose is IEEE senior member.

Erhan Akin received the B. S. degree in electrical engineering from Firat University, Elazig, Turkey, in 1984, the M. S. degree in computer engineering from Firat University, Elazig, Turkey, in 1987, respectively, and the Ph. D. degree in electrical engineering (computer engineering) from Firat University, Elazig, Turkey, in 1994. He is currently an professor doctor in the Department of Computer Engineering, Firat University, Turkey. He is currently the general manager of Firat Technopark and the head of department in Computer Engineering, Firat University. His research interests include soft computing, electric motor drives, fuzzy clusters and systems, nonlinear control systems, fault diagnosis, and computer vision.